

Crystal growth, spectroscopic characteristics, and Judd-Ofelt analysis of Dy: Lu_2O_3 for yellow laser

Jiaojiao Shi(施佼佼), Bin Liu(刘斌), Qingguo Wang(王庆国), Huili Tang(唐慧丽), Feng Wu(吴锋), Dongzhen Li(李东振), Hengyu Zhao(赵衡煜), Zhanshan Wang(王占山), Wen Deng(邓文), Xiaodong Xu(徐晓东), Jun Xu(徐军)
Citation: Chin. Phys. B . 2018, 27(7): 077802. **doi:** 10.1088/1674-1056/27/7/077802

Journal homepage: http://cpb.iphy.ac.cn; http://iopscience.iop.org/cpb

What follows is a list of articles you may be interested in

Transition intensity calculation of Yb: YAG

Hong-Bo Zhang(张洪波), Qing-Li Zhang(张庆礼), Xing Wang(王星), Gui-Hua Sun(孙贵花), Xiao-Fei Wang(王小飞), De-Ming Zhang(张德明), Dun-Lu Sun(孙敦陆)
Chin. Phys. B . 2018, 27(6): 067801. **doi:** 10.1088/1674-1056/27/6/067801

Investigation of europium(Ⅲ)-doped ZnS for immunoassay

Chao-Fan Zhu(朱超凡), Xue Sha(沙雪), Xue-Ying Chu(楚学影), Jin-Hua Li(李金华), Ming-Ze Xu(徐铭泽), Fang-Jun Jin(金芳军), Zhi-Kun Xu(徐志堃)
Chin. Phys. B . 2018, 27(2): 027803. **doi:** 10.1088/1674-1056/27/2/027803

Substitution priority of Eu^{2+} in multi-cation compound $Sr_{0.8}Ca_{0.2}Al_2Si_2O_8$ and energy transfer

Zhi-Ping Yang(杨志平), Zhen-Ling Li(李振玲), Zhi-Jun Wang(王志军), Pan-Lai Li(李盼来), Miao-Miao Tian(田苗苗), Jin-Ge Cheng(程金阁), Chao Wang(王超)
Chin. Phys. B . 2018, 27(1): 017802. **doi:** 10.1088/1674-1056/27/1/017802

Electronic structure and photoluminescence property of a novel white emission phosphor $Na_3MgZr(PO_4)_3:Dy^{3+}$ for warm white light emitting diodes

Ge Zhu(朱革), Zhuo-Wei Li(李卓为), Chuang Wang(王闯), Fa-Guang Zhou(周发光), Yan Wen(温艳), Shuang-Yu Xin(辛双宇)
Chin. Phys. B . 2017, 26(9): 097801. **doi:** 10.1088/1674-1056/26/9/097801

Profile function properties & optical transition formulae

Qing-li Zhang(张庆礼), Guihua Sun(孙贵花), Jin-yun Gao(高进云), Dun-lu Sun(孙敦陆), Jian-qiao Luo(罗建乔), Wen-peng Liu(刘文鹏), De-ming Zhang(张德明), Chaoshu Shi(施朝淑), Shaotang Yin(殷绍唐)
Chin. Phys. B . 2017, 26(7): 077803. **doi:** 10.1088/1674-1056/26/7/077803

Crystal growth, spectroscopic characteristics, and Judd–Ofelt analysis of Dy:Lu_2O_3 for yellow laser*

Jiaojiao Shi(施佼佼)[1,2], Bin Liu(刘斌)[1,2], Qingguo Wang(王庆国)[1,2], Huili Tang(唐慧丽)[1,2,4], Feng Wu(吴锋)[1,2], Dongzhen Li(李东振)[3], Hengyu Zhao(赵衡煜)[1,2], Zhanshan Wang(王占山)[1,2], Wen Deng(邓文)[5], Xiaodong Xu(徐晓东)[3,†], and Jun Xu(徐军)[1,2,6,‡]

[1] *School of Physics Science and Engineering, Institute for Advanced Study, Tongji University, Shanghai* 200092, *China*
[2] *MOE Key Lab of Advanced Micro-Structure Materials, Shanghai* 201899, *China*
[3] *Jiangsu Key Laboratory of Advanced Laser Materials and Devices, School of Physics and Electronic Engineering, Jiangsu Normal University, Xuzhou* 221116, *China*
[4] *State Key Laboratory of Crystal Materials, Shandong University, Jinan* 250100, *China*
[5] *School of Physical Science and Technology, Guangxi University, Guangxi* 530004, *China*
[6] *Shanghai Engineering Research Center for Sapphire Crystals, Shanghai* 201899, *China*

(Received 6 April 2018; revised manuscript received 2 May 2018; published online 25 June 2018)

Dy:Lu_2O_3 was grown by the float-zone (Fz) method. According to the absorption spectrum, the Judd–Ofelt (JO) parameters Ω_2, Ω_4, and Ω_6 were calculated to be 4.86×10^{-20} cm^2, 2.02×10^{-20} cm^2, and 1.76×10^{-20} cm^2, respectively. The emission cross-section at 574 nm corresponding to the $^4F_{9/2}\rightarrow{}^6H_{13/2}$ transition was calculated to be 0.53×10^{-20} cm^2. The yellow ($^4F_{9/2}\rightarrow{}^6H_{13/2}$ transition) to blue ($^4F_{9/2}\rightarrow{}^6H_{15/2}$ transition) intensity ratio ranges up to 12.9. The fluorescence lifetime of the $^4F_{9/2}$ energy level was measured to be 112.1 μs. These results reveal that Dy:Lu_2O_3 is a promising material for use in yellow lasers.

Keywords: fluorescence spectra, laser materials, excited states

PACS: 78.55.–m, 42.70.Hj, 78.47.da **DOI:** 10.1088/1674-1056/27/7/077802

1. Introduction

Rare-earth ion-doped solid-state materials emitting visible laser light, especially in the yellow region, are currently applied in many fields, such as medical treatment, telecommunications, microscopy, and biomedicine.[1,2] Some strategies have been developed to acquire yellow laser light, such as Raman-induced lasing and frequency-doubling lasing in semiconductors. Nevertheless, these methods have some shortcomings, namely high cost, system complexity, and indirect yellow emission. Among rare-earth ions, trivalent dysprosium is suitable for studying luminescent behavior because its $^4F_{9/2}\rightarrow{}^6H_{13/2}$ transition emits yellow light, and the ion is a potential candidate for achieving yellow emission directly and efficiently. In addition, the emergence of the InGaN laser diode (LD) has advanced the study of Dy^{3+}-doped laser materials because it is convenient to pump the $^4I_{15/2}$ level in dysprosium (∼ 446 nm) with an InGaN LD. Up to now, a series of spectral results regarding Dy^{3+}-doped materials have been reported,[3–6] and yellow laser emission from Dy:YAG[7] and Dy,Tb:$LiLuF_4$[8] have been demonstrated.

Lu_2O_3[11] has attracted much attention because of its low phonon energy (430 cm^{-1}), robust thermal stability, and high thermal conductivity.[9,10] However, the high melting point (∼ 2450 °C)[12] of Lu_2O_3 presents a great challenge to its growth. Some methods have been attempted to grow Lu_2O_3 crystals, for example, the heat exchanger method,[13] Czochralski technique,[14] laser-heated pedestal growth,[15] Bridgman method,[16] and micro-pulling technique.[17] However, few Lu_2O_3 crystals with good quality have been obtained for applications. So far, the optical characteristics of Tm^{3+}-,[18] Er^{3+}-,[19] and Yb^{3+}-doped[19] Lu_2O_3 crystals have been investigated. Unfortunately, very few studies were focused on Dy^{3+}-doped Lu_2O_3 crystals.

In this work, crystal growth, spectroscopic properties, and JO theory analysis of Dy:Lu_2O_3 are discussed in detail. Furthermore, we compare the optical characteristics of Dy^{3+}-doped Lu_2O_3 crystals with other materials.

2. Experimental process

Lu_2O_3 (99.99%), Dy_2O_3 (99.99%) powders were used as raw materials and were weighed accurately according to $(Dy_xLu_{1-x})_2O_3$ ($x = 0.03$). The weighed material was mixed

*Project supported by the Fund of Key Laboratory of Optoelectronic Materials Chemistry and Physics, Chinese Academy of Sciences (Grant No. 2008DP173016), the National Key Research and Development Program of China (Grant No. 2016YFB1102202), and the National Key Research and Development Program of China (Grant No. 2016YFB0701002).

†Corresponding author. E-mail: xdxu79@jsnu.edu.cn
‡Corresponding author. E-mail: xujun@mail.shcnc.ac.cn

© 2018 Chinese Physical Society and IOP Publishing Ltd

in a beaker and then shaped into two rods. After pressed at 220 MPa for 3 min, the two rods were sintered in air at 1700 °C for 24 h. One was used as the feed rod and the other was used as the seed rod. The two rods should be placed on a same vertical axis during the growth process. High-purity argon gas was used as a protective atmosphere. The rotation rate and growth rate were set to be 8–12 rpm and 1–2 mm/h for both rods, respectively. After growth, the as-grown Dy:Lu_2O_3 was cooled to room temperature slowly and then annealed in air at 1700 °C for 24 h. A 3 mm×4 mm×1 mm sample was cut and polished for spectral measurements. A photo of the Dy:Lu_2O_3 sample is shown in Fig. 1.

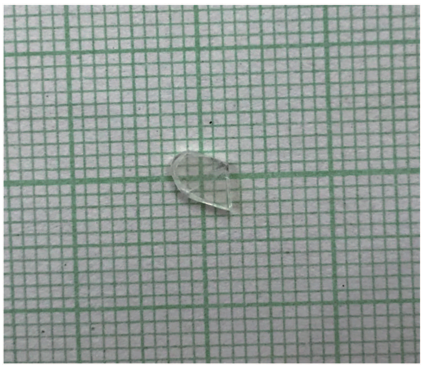


Fig. 1. (color online) The photo of a Dy:Lu_2O_3 sample.

The following measurements were performed at room temperature. XRD analysis of Dy:Lu_2O_3 was performed with an Ultima IV diffractometer (Japan). The absorption spectrum was measured with a Lambda 900 spectrophotometer. The concentration of dysprosium in Dy:Lu_2O_3 was determined to be 2.8 at.% (i.e., 7.99×10^{20} cm^{-3}) using inductively coupled plasma-atomic emission spectrometry (ICP-AES) measurements. The emission spectrum together with the decay curve of Dy:Lu_2O_3 were gathered with a fluorospectrophotometer (FSP920).

3. Results and discussions

The XRD pattern of the Dy:Lu_2O_3 crystal is shown in Fig. 2. The diffraction peaks of Dy:Lu_2O_3 are in accordance with JCPDS 86-2475 of Lu_2O_3, and no impurity peaks can be seen in the spectra. The lattice parameter of Dy:Lu_2O_3 was calculated to be 1.0411 nm, which is similar with that of a pure Lu_2O_3 crystal (1.0391 nm).[30] The results indicate that the obtained Dy:Lu_2O_3 crystal has bixbyite structure with $Ia3$ cubic space group, and the adulteration of Dy^{3+} into Lu_2O_3 does not obviously affect the crystal structure.

The absorption spectrum of Dy^{3+}-doped Lu_2O_3 is presented in Fig. 3, where the corresponding transitions of Dy^{3+} were assigned and marked. As shown in Fig. 3, some absorption bands were overlapped with each other due to the interaction between crystal fields. The absorption cross-section σ_{abs} around 446 nm corresponding to the $^6H_{15/2} \rightarrow {}^4I_{15/2}$ transition was determined to be 0.71×10^{-21} cm^2 with 4.0 nm full width at half maximum (FWHM). These qualities make the Dy:Lu_2O_3 crystal highly desirable for pumping with an InGaN laser diode.[20]

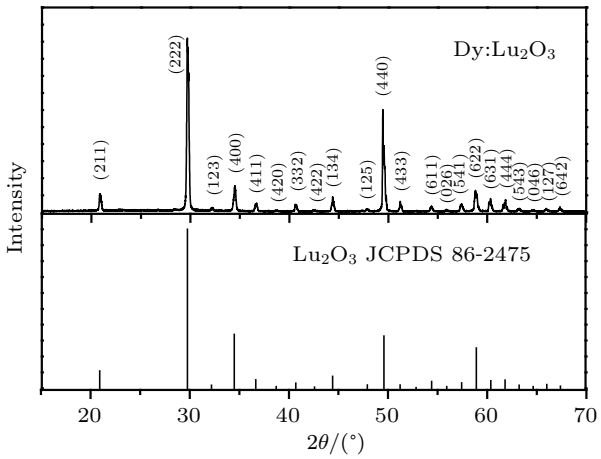


Fig. 2. The XRD pattern of Dy:Lu_2O_3 crystal.

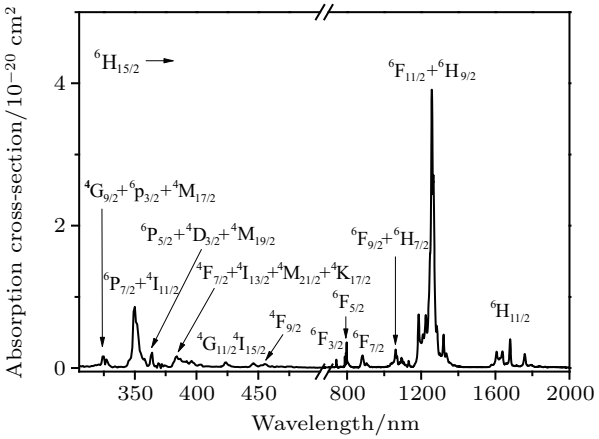


Fig. 3. Absorption spectrum of Dy:Lu_2O_3 crystal.

JO theory[21–23] was used to evaluate the optical characteristics of lanthanide ions doped in host materials in this work. The detailed calculation process used here is the same as that presented in Ref. [2]. The matrix elements for chosen transitions in Dy^{3+} used for calculating the JO parameters were taken from Refs. [32] and [38]. The calculated average wavelength $\overline{\lambda}$, refractive index n,[24] calculated and experimental line strengths (S_{cal} and S_{exp}), and the root-mean-square deviation (rms Δs) are presented in Table 1. The results show that rms $\Delta s = 0.027 \times 10^{-20}$ cm^2, which informs the accuracy of the fitting results. The relatively small value demonstrates that the fitting results between $S_{exp}(J, J')$ and $S_{cal}(J, J')$ are reasonable.

Table 1. The average wavelength ($\bar{\lambda}$), refractive index (n), experimental line strength $S_{\rm exp}(J,J')$, and calculated line strength $S_{\rm cal}(J,J')$ of Dy:Lu_2O_3 crystal.

Transition (from $^6H_{15/2}$)	$\bar{\lambda}$/nm	n	$S_{\rm exp}/10^{-20}$ cm^2	$S_{\rm cal}/10^{-20}$ cm^2
$^6P_{7/2}+^4I_{11/2}$	350	2.009	1.003	1.090
$^6P_{5/2}+^4D_{3/2}+^4M_{19/2}$	364	2.000	0.377	0.417
$^4F_{7/2}+^4I_{13/2}+^4M_{21/2}+^4K_{17/2}$	386	1.987	0.626	0.660
$^4I_{15/2}$	446	1.963	0.130	0.151
$^6F_{5/2}$	795	1.919	0.531	0.608
$^6H_{7/2}+^6F_{9/2}$	1076	1.910	2.472	2.499
$^6H_{9/2}+^6F_{11/2}$	1254	1.906	6.932	6.982
$^6H_{11/2}$	1674	1.900	1.567	1.651
rms $\Delta s/10^{-20}$ cm^2			0.027	

The JO intensity parameters Ω_t ($t = 2, 4, 6$) were obtained through least squares fitting between the calculated and experimental line strength. The JO intensity parameters Ω_t ($t = 2, 4, 6$) of Dy^{3+}-doped Lu_2O_3 and other hosts are presented in Table 2. The calculated Ω_2, Ω_4, and Ω_6 values of Dy:Lu_2O_3 are 4.86×10^{-20} cm^2, 2.02×10^{-20} cm^2, and 1.76×10^{-20} cm^2, respectively. Normally, Ω_2 is related to the asymmetry of the crystal field and matrix environment around lanthanide ions. The value of Ω_2 is proportional to the asymmetry and is inversely proportional to the contravalency. Ω_4/Ω_6 is used as a spectroscopic quality factor and is a significant characteristic parameter for estimating the stimulated emission efficiency.[27] As shown in Table 2, the value of Ω_4/Ω_6 for Dy:Lu_2O_3 is larger than that for most other crystals, revealing that Dy:Lu_2O_3 is an excellent candidate for laser emission. The radiative lifetime $\tau_{\rm rad}$, fluorescence branching ratio β and spontaneous radiation transition probability A for a Dy:Lu_2O_3 crystal were calculated, and the results are shown in Table 3. In a Dy:Lu_2O_3 crystal, the $^4F_{9/2}\rightarrow{}^6H_{13/2}$ transition shows the largest fluorescence branching ratio of 61.19%, which indicates a high possibility of yellow emission around 574 nm. Moreover, the radiative lifetime $\tau_{\rm rad}$ of Dy:Lu_2O_3 (756 μs) is comparable to Dy:YAP (757 μs)[2] and is larger than that of Dy:$CaGdAlO_4$ (501 μs),[27] Dy:$Li_3Ba_2La_3(MoO_4)_8$ (215 μs),[28] and Dy:$NaGd(WO_4)_2$ (281 μs),[35] indicating Dy:Lu_2O_3 has excellent energy storage capability.

Table 2. The J–O intensity parameters with Ω_4/Ω_6 values for different Dy^{3+}-doped crystals.

Hosts	$\Omega_2/10^{-20}$ cm^2	$\Omega_4/10^{-20}$ cm^2	$\Omega_6/10^{-20}$ cm^2	Ω_4/Ω_6	Ref.
$CaGdAlO_4$	1.80	1.00	0.50	2.00	[27]
YSGG	0.13	0.73	1.06	0.68	[25]
K_2GdF_5	2.51	0.94	2.12	0.44	[26]
$LiNbO_3$	5.42	1.14	2.51	0.45	[29]
$ZnWO_4$	7.76	0.57	0.31	1.84	[31]
$LiYF_4$	2.01	1.34	2.39	0.89	[32]
YAG	0.20	1.11	1.46	0.76	[36]
YAP	3.93	1.64	3.79	0.43	[2]
$LiLuF_4$	2.04	0.91	1.09	0.83	[37]
Lu_2O_3	4.86	2.02	1.76	1.15	This work

Table 3. Spontaneous emission transition probability A, fluorescence branching ratio β, and radiative lifetime $\tau_{\rm rad}$ of Dy:Lu_2O_3 crystal.

Transitions		A/s^{-1}	β/%
$^4F_{9/2}\rightarrow$	$^6F_{5/2}$	17.005	1.29
	$^6F_{7/2}$	9.904	0.75
	$^6H_{5/2}$	6.062	0.46
	$^6H_{7/2}$, $^6F_{9/2}$	42.341	3.20
	$^6H_{9/2}$, $^6F_{11/2}$	51.371	3.88
	$^6H_{11/2}$	107.858	8.15
	$^6H_{13/2}$	809.418	61.19
	$^6H_{15/2}$	278.911	21.08
Radiative lifetime/μs	$\tau_{\rm rad} = 756$		

The emission spectrum of Dy:Lu_2O_3 under 446 nm excitation is shown in Fig. 4. The $^4F_{9/2}\rightarrow{}^6H_{9/2}+{}^6F_{11/2}$, $^6H_{11/2}$, $^6H_{13/2}$, and $^6H_{15/2}$ transitions are centered at 487 nm, 574 nm, 673 nm, and 761 nm, respectively. Among these transitions, the $^4F_{9/2}\rightarrow{}^6H_{13/2}$ transition at 574 nm exhibits the largest intensity, which agrees well with the JO theory results shown in Table 3. Near 574 nm, the emission cross-section $\sigma_{\rm em}$ and FWHM are 0.53×10^{-20} cm^2 and 2.69 nm, respectively. The corresponding $\sigma_{\rm em}$ of Dy:Lu_2O_3 is larger than that of Dy:YAP[2] and is comparable to those of Dy:$GdVO_4$[33] and Dy:$ZnWO_4$[31] with a magnitude of 10^{-20} cm^2. For the $^4F_{9/2}\rightarrow{}^6H_{13/2}$ and $^4F_{9/2}\rightarrow{}^6H_{15/2}$ transitions in Dy^{3+}, the intraconfigurational transitions split into maximum number energy levels,[39] which have a more important influence on the luminescence than other transitions. Thus, we compared the $^4F_{9/2}\rightarrow{}^6H_{15/2}$ transition (blue emission) with the

$^4F_{9/2} \rightarrow {}^6H_{13/2}$ transition (yellow emission). The yellow to blue intensity ratio (Y/B) is an important parameter of reflecting the possibility of yellow laser emission. A large Y/B value indicates a material is more likely to emit yellow laser light.[27,28] To the best of our knowledge, it has been reported that the emission from Dy:LTT was yellowish-white, which is primarily due to its large Y/B value.[40] For the Dy:Lu_2O_3 crystal, the yellow ($^4F_{9/2} \rightarrow {}^6H_{13/2}$ transition around 574 nm) to blue ($^4F_{9/2} \rightarrow {}^6H_{15/2}$ transition around 487 nm) intensity ratio is 12.9, which is relatively larger than that in Dy:$Li_3Ba_2La_3(MoO_4)_8$ (4.52),[28] Dy:$YAl_3(BO_3)_4$ (3.37),[29] and Dy:$CaGdAlO_4$ (3.68).[27]

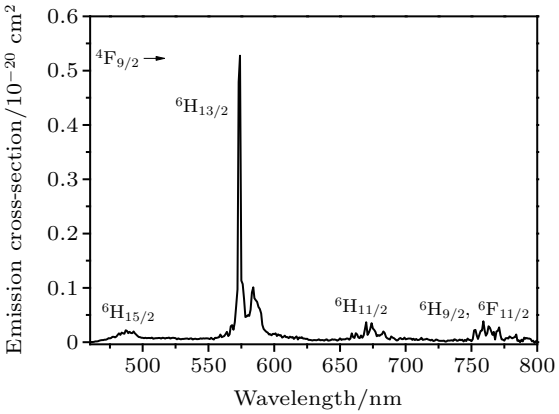


Fig. 4. Emission spectrum of Dy:Lu_2O_3 crystal.

The fluorescence decay curve of the $^4F_{9/2}$ multiplet under 446 nm excitation is presented in Fig. 5. The fluorescence lifetime τ was measured to be 112.1 μs. Thus, the fluorescence quantum efficiency η ($\eta = \tau/\tau_{rad}$) is 14.8%. This result is principally caused by the high concentration (7.99×10^{20} cm^{-3}) of Dy^{3+} in Lu_2O_3. The increased concentration will arouse cross-relaxations of Dy^{3+} via $^4F_{9/2}+{}^6H_{15/2}$ to $({}^6F_{3/2}, {}^6F_{1/2})+({}^6H_{9/2}, {}^6F_{11/2})$.[34] It has been reported that the fluorescence quantum efficiency changed from 94.3% to 5.5% as the concentration of Dy^{3+} increases from 0.4 at.% to 15.0 at.% in a Dy:$LiLa(MoO_4)_2$ crystal.[34] Therefore, the quantum efficiency of Dy:Lu_2O_3 would be optimized by altering the doped concentration of Dy^{3+}.

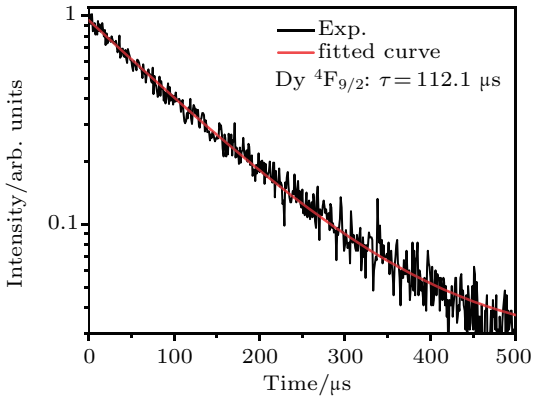


Fig. 5. (color online) Fluorescence decay curve of the $^4F_{9/2}$ level in a Dy:Lu_2O_3 crystal.

A comparison of the optical parameters in different Dy^{3+}-doped hosts is shown in Table 4. Among them, yellow laser emission has been observed in Dy:YAG and Dy, Tb:$LiLuF_4$. As for Dy:$LiNbO_3$ crystals, gain of the yellow transition has also been realized. As shown in Table 4, the absorption cross-section σ_{abs} corresponding to $^6H_{15/2} \rightarrow {}^4I_{15/2}$ transition of Dy:Lu_2O_3 is smaller than that of Dy:YAG and Dy:$LiLuF_4$, but is larger than that of Dy:$LiNbO_3$. The emission cross-section σ_{em} corresponding to $^4F_{9/2} \rightarrow {}^6H_{13/2}$ transition of Dy:Lu_2O_3 is larger than that of Dy:YAG, Dy:$LiLuF_4$, and Dy:$LiNbO_3$ near 574 nm, indicating that Dy:Lu_2O_3 is beneficial for high gain and low threshold laser emission. The fluorescence branching ratio β of Dy:Lu_2O_3 is larger than that of YAG (50.96%) and is comparable to that of $LiLuF_4$ (65.40%) and $LiNbO_3$ (65.50%). The above data reveal that Dy:Lu_2O_3 is quite promising for yellow laser emission.

Table 4. A comparison of absorption wavelength and absorption cross-section σ_{abs} for the $^6H_{15/2} \rightarrow {}^4I_{15/2}$ transition, emission wavelength, fluorescence branching ratio β, and emission cross-section σ_{em} for the $^4F_{9/2} \rightarrow {}^6H_{13/2}$ transition in different Dy^{3+}-doped hosts.

Hosts	Absorption Wavelength/nm	$\sigma_{abs}/10^{-21}$ cm^2	Emission Wavelength/nm	$\sigma_{em}/10^{-20}$ cm^2	β/%	Ref.
YAG	447	1.60	582	0.30	50.96	[7], [36]
$LiLuF_4$	447	0.98	574	0.45	65.40	[8], [37]
$LiNbO_3$	–	0.60	574	0.32	65.50	[31]
Lu_2O_3	446	0.71	574	0.53	61.19	This work

4. Conclusion

In conclusion, a Dy:Lu_2O_3 single crystal was successfully grown via the Fz method. The optical properties and JO analysis were studied in detail. The XRD diffraction peaks of Dy:Lu_2O_3 are in accordance with JCPDS 86-2475. The absorption cross-section and FWHM near 446 nm were found to be 0.71×10^{-21} cm^2 and 4.0 nm, respectively. Based on the absorption spectrum, the JO intensity parameters Ω_t (t = 2, 4, 6) were calculated to be $\Omega_2 = 4.86 \times 10^{-20}$ cm^2, $\Omega_4 = 2.02 \times 10^{-20}$ cm^2, and $\Omega_6 = 1.76 \times 10^{-20}$ cm^2, respectively. The Y/B value ranges up to 12.9, reflecting the possibility of yellow laser emission. The emission cross-section and

FWHM near 574 nm were found to be 0.53×10^{-20} cm^2 and 2.69 nm, respectively. The fluorescence lifetime corresponding to the $^4F_{9/2} \rightarrow {}^6H_{13/2}$ emission line at 574 nm was fitted to be 112.1 μs. Through the above analysis, Dy:Lu_2O_3 crystal could be a promising material for yellow laser emission.

References

[1] Wang Y N, Zheng Q, Yao Y and Chen X 2013 *Appl. Opt.* **52** 1876
[2] Liu B, Shi J J, Wang Q G, Tang H L, Liu J F, Zhao H Y, Li D Z, Liu J, Xu X D, Wang Z S and Xu J 2017 *Opt. Mater.* **72** 208
[3] Zhang Y, Xu J and Lu B 2014 *J. Alloy. Comp.* **582** 635
[4] Singh V, Jun-Jie Z, Rao T K G, Tiwari M and Hong-Cheng P 2005 *Chin. Phys. Lett.* **22** 3182
[5] Haro-González P, Martín L L, Martín I R, Berkowski M and Ryba-Romanowski W 2011 *Appl. Phys. B* **103** 597
[6] Zhu G, Li Z W, Wang C, Zhou F G, Wen Y and Xin S Y 2017 *Chin. Phys. B* **26** 097801
[7] Bowman S R, O'Connor S and Condon N J 2012 *Opt. Express* **20** 12906
[8] Bolognesi G, Parisi D, Calonico D, Costanzo G A, Levi F, Metz P W, Krankel C, Huber G and Tonelli M 2014 *Opt. Lett.* **39** 6628
[9] Griebner U, Petrov V, Petermann K and Peters V 2004 *Opt. Express* **12** 3125
[10] Peters R, Kränkel C, Petermann K and Huber G 2007 *Opt. Express* **15** 7075
[11] Pauling L and Shappell M D 1930 *Z. Kristallogr.* **75** 128
[12] Coutures J P, Verges R and Foex M 1975 *Rev. Int. Hautes Temp. Réfract.* **12** 181
[13] Fornasiero L, Mix E, Peters V, Petermann K and Huber G 1999 *Cryst. Res. Technol.* **34** 255
[14] Fornasiero L, Mix E, Peters V, Petermann K and Huber G 2000 *Ceram. Int.* **26** 589
[15] Laversenne L, Guyot Y, Goutaudier C, Cohen-Adad M T and Boulon G 2001 *Opt. Mater.* **16** 475
[16] Petermann K, Fornasiero L, Mix E and Peters V 2002 *Opt. Mater.* **19** 67
[17] Mun J H, Jouini A, Novoselov A, Guyot Y, Yoshikawa A, Ohta H, Shibata H, Waseda Y, Boulon G and Fukuda T 2007 *Opt. Mater.* **29** 1390
[18] Fukabori A, Chani V, Kamada K, Moretti F and Yoshikawa A 2011 *Cryst. Growth* . **11** 2404
[19] McMillen C, Thompson D, Tritt T and Kolis J 2011 *Cryst. Growth* . **11** 4386
[20] Nakamura S, Senoh M, Nagahama S I, Iwasa N, Yamada T, Matsushita T and Sugimoto Y 1996 *Jpn. J. Appl. Phys.* **35** 74
[21] Judd B R 1962 *Phys. Rev.* **127** 750
[22] Ofelt G S 1962 *J. Chem. Phys.* **37** 511
[23] Wang Y, Li J, Tu C, You Z, Zhu Z and Wu B 2007 *Cryst. Res. Technol.* **42** 1063
[24] Kaminskii A A, Akchurin M S, Becker P, Ueda K, Bohatý L, Shirakawa A, Tokurakawa M, Takaichi K, Yagi H, Dong J and Yanagitani T 2008 *Laser Phys. Lett.* **5** 300
[25] Sardar D K, Bradley W M, Yow R M, Gruber J B and Zandi B 2004 *J. Lumin.* **106** 195
[26] Van Do P, Tuyen V P, Quang V X, Thanh N T, Ha V T T, Tuyen H V, Khaidukov N M, Marcazzo J, Lee Y and Huy B T 2013 *Opt. Mater.* **35** 1636
[27] Xu X D, Hu Z W, Li R J, Li D Z, Di J Q, Su L B, Yang Q H, Sai Q L, Tang H L, Wang Q G, Strzęp A and Xu J 2017 *Opt. Mater.* **66** 469
[28] Song M, Wu M, Zhou W, Zhou X, Wei B and Wang G 2014 *J. Alloy. Comp.* **607** 110
[29] Ryba-Romanowski W, Dominiak-Dzik G, Solarz P and Lisiecki R 2009 *Opt. Mater.* **31** 1547
[30] Peters V 2001 *Growth and Spectroscopy of Ytterbium-doped Sesquioxides* (Ph.D. Thesis) (Hamburg: Universität Hamburg)
[31] Yang F, Tu C, Wang H, Wei Y, You Z, Jia G and Wang Y 2007 *Opt. Mater.* **29** 1861
[32] Brik M G, Ishii T, Tkachuk A M, Ivanova S E and Razumova I K 2004 *J. Alloys Comp.* **374** 63
[33] Ning K J, He X M, Zhang L H, Liu Y C, Yin J G, Zhang P X, Chen G Z, wang X Y, Chen Z, Shi C J, Hong J Q and Hang Y 2014 *Opt. Mater.* **37** 745
[34] Zhao W, Zhou W W, Wei B, Yu Y, Wang G F, Du J M, Yu H J, Lv Z C and Chen Y H 2012 *J. Alloy. Comp.* **538** 136
[35] Wang H, Li J, Jia G, You Z, Yang F, Wei Y, Wang Y, Zhu Z, Lu X and Tu C 2007 *J. Lumin.* **126** 452
[36] Lupei A, Lupei V, Gheorghe C, Ikesue A and Enculescu M 2011 *J. Appl. Phys.* **110** 083120
[37] Bigotta S, Tonneli M, Cavalli E and Belletini A 2010 *J. Lumin.* **130** 13
[38] Carnall W T, Fields P R and Rajnak K 1968 *J. Chem. Phys.* **49** 4424
[39] Jayasimhadri M, Ratnam B V, Jang K and Lee H S 2010 *J. Am. Ceram. Soc.* **93** 494
[40] Babu A M, Jamalaiah B C, Kumar J S, Sasikala T and Moorthy L R 2011 *J. Alloys Comp.* **509** 457